

RSC Advances



This article can be cited before page numbers have been issued, to do this please use: Z. Jia, W. Yuan, H. Zhao, H. hu and G. L. Baker, *RSC Adv.*, 2014, DOI: 10.1039/C4RA07262F.

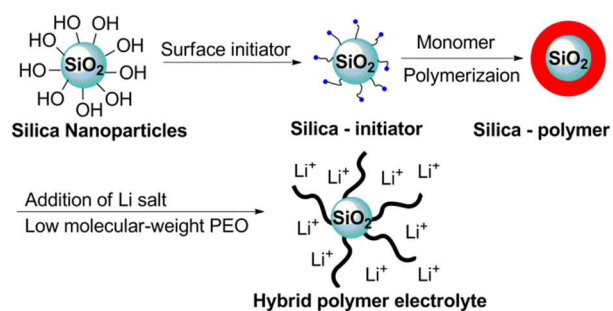


This is an *Accepted Manuscript*, which has been through the Royal Society of Chemistry peer review process and has been accepted for publication.

Accepted Manuscripts are published online shortly after acceptance, before technical editing, formatting and proof reading. Using this free service, authors can make their results available to the community, in citable form, before we publish the edited article. This *Accepted Manuscript* will be replaced by the edited, formatted and paginated article as soon as this is available.

You can find more information about *Accepted Manuscripts* in the [Information for Authors](#).

Please note that technical editing may introduce minor changes to the text and/or graphics, which may alter content. The journal's standard [Terms & Conditions](#) and the [Ethical guidelines](#) still apply. In no event shall the Royal Society of Chemistry be held responsible for any errors or omissions in this *Accepted Manuscript* or any consequences arising from the use of any information it contains.



This work reported an extensive study of poly(ethylene oxide)-containing polymers grafted silica nanoparticles and their performance as polymer composite electrolytes

Composite Electrolytes Comprised of Poly(Ethylene Oxide) and Silica Nanoparticles
with Grafted Poly(Ethylene Oxide)-Containing Polymers

Zhe Jia, Wen Yuan, Hui Zhao, Heyi Hu, Gregory L. Baker[§]

Department of Chemistry, Michigan State University, East Lansing, Michigan 48824,
United States

Correspondence to: Zhe Jia (jiazhe@msu.edu)

§ Prof. Gregory L. Baker passed away on October 18, 2012. We dedicate this work as a
memorial to him

Abstract

We designed, synthesized and characterized several novel hybrid inorganic/organic nanocomposite electrolytes that consist of poly(ethylene oxide) (PEO) based polymer grafted from silica nanoparticles. Poly(ethylene glycol) methyl ether methacrylate (PEGMA) was tailored on the silica surface through atom transfer radical polymerization (ATRP). A series of silica-polymers were synthesized with different length of PEO side chains. Electrolytes were prepared from the functionalized particles and low-molecular weight polyethylene glycol dimethyl ether (PEGDME) with the addition of LiI. Upon the introduction of particles, electrolytes became viscous and gel-like. With the increase of PEO side chains, viscosity of the electrolytes increased dramatically, among which, silica-poly(PEGMA-1100) became solid-state. The room temperature conductivity of hybrid silica-polymer electrolytes are in the range of 6×10^{-5} to 1.2×10^{-4} S/cm. Silica-poly(PEGMA-475) and silica-poly(PEGMA-1100), with higher viscosity, represented better ionic conductivity. Surface-initiated copolymerization was also conducted to optimize the electrochemical performance of polymer coated silica nanoparticles.

Keywords

Composite electrolyte; surface-initiated ATRP; poly(ethylene glycol) methyl ether methacrylate; conductivity

1 Introduction

The development of sustainable energy-harvesting devices is perhaps the most crucial technological challenge for mankind,^{1,2} and dye-sensitized solar cells (DSSCs)³⁻⁵ and rechargeable lithium ion batteries (LIBs)⁶⁻⁸ represent important advances in this area. Electrolytes that carry charge between the electrodes of these systems strongly affect device construction and efficiency.⁹ Of particular relevance to this work, difficulties in sealing liquid electrolytes in batteries or solar cells and safety issues raised during device operation are driving the development of solid-state electrolytes.¹⁰ One approach for creating highly conductive solid electrolytes employs organic/inorganic nanocomposite materials, which often combine the advantages of both organic and inorganic components.^{11, 12} These nanocomposites usually have core-shell architectures comprised of organic polymer shells and inorganic nanoscale cores, to combine the flexibility, and processability of organic polymers with the rigidity and thermal stability of the inorganic component.¹³

Among the candidates for replacing conventional liquid electrolytes, poly(ethylene oxide) (PEO) based polymers are particularly attractive for LIBs,¹⁴ DSSCs,¹⁵ fuel cells¹⁶ and other solid-state electrochemical devices because these polymers are relatively stable and dissolve high levels of salts due to their high polarity.¹⁷ In 1973, Wright first studied the ionic conductivity of PEO-alkali metal salt complexes.¹⁸ Since that time, many groups worked to develop PEO and its derivative polymers as stable and highly conducting solid polymer electrolytes. However, the ion conduction only occurs in the amorphous PEO phase, where conductivity is two to three orders of magnitude higher than in the crystalline phase,¹⁹ so the ionic conductivities of common

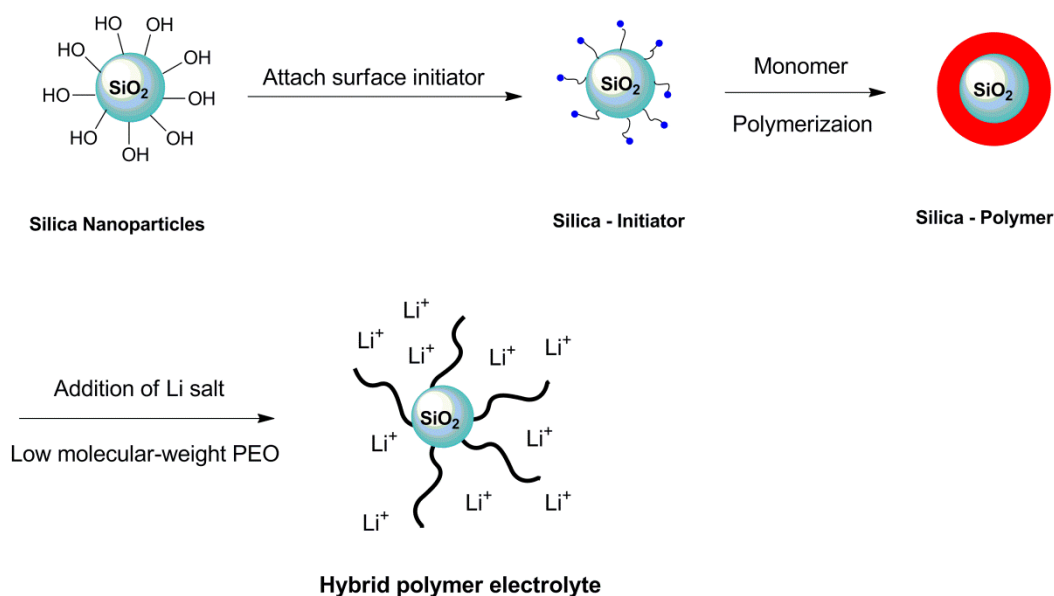
PEO-salt systems are not satisfactory because of PEO crystallization.²⁰ Improvements in conductivity require the introduction of disorder to prevent crystallization,²¹ and approaches to this end including blending polymers, cross-linking, copolymerization, and plasticizer addition.^{17, 22}

With the development of controlled living radical polymerization, including atom transfer radical polymerization (ATRP),²³⁻²⁶ reversible addition-fragmentation chain transfer radical polymerization (RAFT)²⁷⁻³⁰ and nitroxide-mediated polymerization (NMP)³¹⁻³⁴, the scope of surface modification with polymers increased dramatically. Researchers have synthesized numerous inorganic/organic composite materials with tailored polymer shells coated on inorganic cores.³⁵ After anchoring an initiator to the target surface, initiation of polymerization leads to a dense layer of immobilized polymer via a “grafting from” approach.³⁶⁻³⁸ Our lab invoked controlled living radical polymerization to grow customized polymers from silica³⁹ and gold.⁴⁰

The research described here examines the hypothesis that utilizing controlled polymerization of optimized PEO-based polymers from silica nanoparticles and incorporation of these particles in pure PEO with metal salts will lead to solid or highly viscous materials with high conductivity. The nanoparticle should enhance mechanical strength and may inhibit PEO crystallization to increase conductivity. Grafted copolymers with a significant fraction of short PEG side chains should also lead to a decreased crystallization and increased conductivity.

Scheme 1 shows the synthesis of modified electrolytes and their incorporation in PEO. We synthesized several hybrid inorganic/organic electrolytes by first polymerizing poly(ethylene glycol) methyl ether methacrylate (PEGMA) from silica nanoparticles via

surface-initiated ATRP. The hydroxyl groups on the surface of the silica particles afford sites for initiator attachment and subsequent PEGMA growth, and grafting of both homopolymers and copolymers from particle surfaces occurs with controlled growth rates and thicknesses. Corresponding free polymers were synthesized in solution via ATRP to monitor macromolecule behavior.



Scheme 1 Surface-initiated polymerization from a silica nanoparticle and subsequent formation of a composite electrolyte

One of the target applications of these nanocomposite PEGMA electrolytes is DSSCs, so we selected LiI as the lithium source during electrolyte preparation. The Γ^-/I_3^- redox couple is the most common system employed to regenerate dyes in DSSCs. Thus, we prepared electrolytes from the functionalized particles and low-molecular weight polyethylene glycol dimethyl ether (PEGDME) with the addition of LiI and I_2 . Upon the introduction of particles in PEGDME, electrolytes formed gels, and with the increasing

length of PEO side chains in grafted polymers, the viscosity of the electrolytes increased dramatically. Some electrolytes solidified. Surprisingly, electrolytes containing longer PEO side chains show higher ionic conductivity than electrolytes with shorter side chains on the silica coated particles, despite much lower viscosity with shorter side chains. Surface-initiated copolymerization allows optimization of the ion conductivity of the composite electrolytes via prevention of crystallization. Conductivity values for hybrid silica-copolymer electrolytes ranged from 1.1×10^{-4} to 1.5×10^{-4} S/cm, an order-of-magnitude improvement compared to the homopolymer-coated silica particle electrolytes, and very close to the conductivity of free poly(PEGMA) electrolytes, which have much lower viscosity. The high viscosity of the hybrid electrolytes is attractive for their encapsulation.

2 Experimental

2.1 Materials

Lithium iodide (crystalline powder, 99.9%), cetyltrimethylammonium bromide (CTAB), copper (I) bromide (CuBr, 99.999%), ethyl 2-bromoisobutyrate (EBiB, 98%), methacryloyl chloride (97%), 10-undecen-1-ol (98%), 2-bromoisobutyryl bromide (98%), trichlorosilane (99%), tri(ethylene glycol) monomethyl ether (96%), and di(ethylene glycol) monomethyl ether (96%) were obtained from Aldrich and used as received. N, N, N', N'-ethylenediaminetetraacetic acid (disodium salt dehydrate, EDTA·2Na) was purchased from Spectrum. Triethylamine and hydroquinone were obtained from J. T. Baker Chemical and used as received. Iodine (Aldrich, 99.99%) and 2, 2'-bipyridine (bpy, Aldrich, 99%) were sublimed prior to use. Poly(ethylene glycol) methyl ether

methacrylates (Aldrich, average $M_n=300$, 475, or 1100) were passed through an activated basic alumina column before use. Snowtex-XS (7-10 nm) was a gift from Nissan Chemical, and the colloidal silica was received as an aqueous dispersion in pH 9-10 water. All other chemicals and solvents were ACS reagent grade and used as received from commercial suppliers without further purification unless otherwise specified.

2.2 Instruments

^1H NMR spectra were obtained using Varian Inova 500 MHz instruments. Thermogravimetric analyses (TGA) were performed in air using a Perkin-Elmer TGA 7 Instrument, with a heating rate of 10 °C/min; samples were heated up to 850 °C after holding at 120 °C for 30 min prior to the temperature ramp. FT-IR spectra were collected with a Mattson Galaxy 300 spectrometer through KBr pellets. Differential scanning calorimetry (DSC) was carried out using a TA DSC Q100 instrument with a heating/cooling/heating cycle of 10 °C/min under nitrogen. Transmission electron microscopy (TEM) images were obtained with a high resolution JEOL100 CXII instrument with both digital and film image recording capabilities. Samples were spotted on copper grids coated with ultrathin polymer films (PELCO® TEM grid 01822). Electrical impedance spectroscopy (EIS) analysis was done with a Hewlett-Packard 4192A LF Impedance Analyzer to obtain temperature-dependent ionic conductivity data. Electrolytes were pipetted into a cell and resistance measurements were taken when voltage was passed through the cell at 5 °C intervals from 30-90 °C. The sample cell uses two steel disks as symmetrical electrodes separated by a sample 0.6 cm in radius and 0.02 cm in thickness. The EIS testing apparatus were placed inside a N_2 -filled glove box and all measurements were conducted inside the glove box to avoid moisture.

2.3 Synthesis and characterization of initiator-coated silica nanoparticles (silica-initiator)

Preparation of silica-initiator nanoparticles. Particle preparation followed a literature procedure.³⁹ 1 g of cetyltrimethylammonium bromide (CTAB) was added into 20 mL of Snowtex-XS, and the mixture was stirred at room temperature for 30 min, during which the particles aggregated and precipitated from solution. Silica particles were collected by centrifugation and were then redispersed in 100 mL deionized water to remove CTAB residues. Particles were recollected by centrifugation, and the collecting/redispersing process was repeated 20 times to remove CTAB as completely as possible. Finally, silica particles were dried under high vacuum (10 mTorr) at 70 °C overnight.

(11-(2-bromo-2 methyl) propionyloxy)undecyl-trichlorosilane was synthesized via a two-step literature procedure.⁴¹ 10-undecen-1-ol (1.71g, 10mmol) and pyridine (0.96 mL, 12 mmol) were dissolved in 10 ml of distilled THF, followed by the addition of 2-bromoisobutryl bromide (1.24 mL, 10 mmol) drop by drop over a period of 10 minutes. The mixture was stirred at room temperature under N₂ atmosphere overnight. Following dilution with 20 mL hexane, and washing with 3N HCl three times and distilled water three times, the organic phase obtained was dried over Na₂SO₄ and filtered under reduced pressure. Finally, solvent was removed and a colorless oily liquid product, 10-undecen-1-yl 2-bromo-2-methylpropionate, was obtained (2.63 g, 82.5% yield). ¹H NMR (500 MHz, CDCl₃): δ 1.22 – 1.41 (m, 12H), 1.60 – 1.70 (m, 2H), 1.92 (s, 6H), 1.97 – 2.06 (m, 2H), 4.15 (t, 2H), 4.86 – 5.02 (m, 2H), 5.85 – 5.72(m, 1H).

10-undecen-1-yl 2-bromo-2-methylpropionate (2 g, 6.27 mmol) and trichlorosilane (5 mL, 50.7 mmol) were added into a flame-dried flask, followed by the addition of Karstedt's catalyst (10 μ L). The reaction took place at room temperature overnight under N_2 , and, the mixture was passed through a flash column to remove catalyst. Excess trichlorosilane was removed by vacuum distillation (60 $^{\circ}$ C, 100 mTorr), to give a colorless oil, (11-(2-Bromo-2-methyl)propionyloxy) undecyltrichlorosilane (1.81 g, 72% yield). 1H NMR (500 MHz, $CDCl_3$): δ 1.21 – 1.41 (t, 2H), 1.46 – 1.75 (m, 4H), 1.92 (s, 6H), 4.15 (t, 2H).

Freshly prepared surface initiator, (11-(2-bromo-2 methyl) propionyloxy)undecyltrichlorosilane, was dissolved in dry toluene, and stirred with silica nanoparticles under N_2 at 60 – 70 $^{\circ}$ C overnight. Initiator was in excess to ensure effective anchoring onto the surface of the silica nanoparticles. The initiator-coated particles were collected by centrifugation, dispersed into toluene, washed with pentane, and then recollected by centrifugation. The redispersion /wash/centrifugation/recollecting cycle was repeated at least 10 times to remove any free initiator from the solution or particle surface. The initiator-coated nanoparticles were finally dried under vacuum (10 mTorr) at 70 $^{\circ}$ C overnight.

Calculation of initiator content grafted on silica-initiator nanoparticles. After drying, TGA was conducted to determine the amount of initiator attached to the particles. TGA was performed under a dry air atmosphere, holding the temperature at 120 $^{\circ}$ C for 30 min before starting the temperature ramp at 10 $^{\circ}$ C/min up to 850 $^{\circ}$ C. The TGA data showed 23.7% weight loss, implying that 1 mg of initiator-coated nanoparticles contained 0.237 mg initiator. The molar mass of the initiator is 342.54 g/mol, so there is 6.9×10^{-7}

mole of initiator per mg of silica-initiator. Thus, when surface-initiated ATRP was conducted with 62 mg of initiator coated particles, the solution contained 0.042 mmol of initiator. Therefore, for each surface-initiated ATRP reaction, the monomer (2 mmol) to initiator ratio was roughly 47:1.

2.4 Surface-initiated ATRP of silica-poly(PEGMA) homopolymers

Synthesis of tri(ethylene glycol) methyl ether methacrylate.⁴² Tri(ethylene glycol) monomethyl ether (13.7 g) and 20 mL of triethylamine (0.14 mol) were dissolved in 50 mL of diethyl ether in a three-neck round-bottom flask and placed in an ice bath. To this flask a solution containing 6.87 mL of methacryloyl chloride (0.07 mol) in 15 mL of ethyl ether was added dropwise over 15 minutes. The reaction was allowed to proceed overnight at room temperature under N₂. The mixture was filtered under reduced pressure to remove the precipitate, and the residue was purified by silica gel column chromatography (hexanes/ethyl acetate 1/2, v/v). After removal of the solvent, a small amount (ca. 3 mg) of hydroquinone was added to the product as a polymerization inhibitor. The product was further purified by vacuum distillation at 120 °C, 100 mTorr to obtain a colorless liquid (11.29 g, 70% yield). ¹H NMR (500 MHz, CDCl₃): δ 1.92 (s, 3H), 3.37 (t, 3H), 3.64 (m, 10H), 4.28 (t, 2H), 5.55 (s, 1H), 6.11 (s, 1H).

Synthesis of di(ethylene glycol) methyl ether methacrylate.⁴² This synthesis followed the same protocol described with the same molar ratios of reactants to obtain a colorless liquid (78% yield). ¹H NMR (500 MHz, CDCl₃): δ 1.93 (s, 3H), 3.36 (t, 3H), 3.64 (m, 8H), 4.28 (t, 2H), 5.55 (t, 1H), 6.11 (q, 1H).

Surface-initiated ATRP of tri(ethylene glycol) methyl ether methacrylate (Silica-poly(PEGMA-232)).¹¹ The monomer was first dissolved in methanol and passed

through an activated basic alumina column to remove inhibitor. After removing the methanol, 0.464 g of tri(ethylene glycol) methyl ether methacrylate (2 mmol), 28 mg of 2,2-bipyridine (bpy, 0.18 mmol), and 62 mg of initiator grafted-particles (ca. 0.042 mmol of initiators) were dissolved or dispersed in 1 mL of deionized water and 3 mL of methanol in a Schlenk flask. The mixture was ultrasonicated for 15-20 minutes. After 3 freeze-pump-thaw cycles, the Schlenk flask was filled with nitrogen, and 8 mg of CuBr (0.06 mmol) was added to the mixture, which became dark brown. After another freeze-pump-thaw cycle, the reaction was allowed to take place at room temperature for 12 hours. To quench the reaction, the Schlenk flask was opened and exposed to air, and the solution turned blue. The mixture was transferred to a 50-mL centrifuge tube and washed with an EDTA•2Na-saturated solution several times, until no blue color was observed. Subsequent washes employed deionized water 10 times and acetone 3 times. In each step the polymer-grafted silica particle was recollected by centrifugation. The product was dried under vacuum (≤ 10 mTorr) at 70 °C overnight. After drying, TGA was performed to determine the extent of polymer grafting on the particles.

Surface-initiated ATRP of silica-poly(PEGMA-188), silica-poly(PEGMA-300), silica-poly(PEGMA-475), and silica-poly(PEGMA-1100) followed the same protocol with 2 mmol of monomer in the polymerization solution in all cases.

2.5 Surface-initiated ATRP of silica-copolymer

Surface-initiated ATRP of Silica-Copolymer-1 (Silica-poly(PEGMA-1100-co-PEGMA-232), 1:1). Two monomers for copolymerization, PEGMA-1100 and PEGMA-232, were dissolved separately in methanol and passed through an activated basic alumina to remove inhibitor. Copolymerization of PEGMA-1100 and PEGMA-232 at a

1:1 monomer ratio was carried out via surface-initiated ATRP. Initially, 1.1 g of poly(ethylene glycol) methyl ether methacrylate ($M_n=1100$, 1 mmol, PEGMA-1100), 0.232 g of tri(ethylene glycol) methyl ether methacrylate (1 mmol, PEGMA-232), 28 mg of 2, 2-bipyridine (bpy, 0.18 mmol), and 62 mg of initiator-modified particles (ca. 0.042 mmol) were dissolved or dispersed in 1 mL of deionized water and 3 mL of methanol in a Schlenk flask. The mixture was ultrasonicated for 15-20 minutes. After 3 freeze-pump-thaw cycles the Schlenk flask was filled with N_2 , and 8 mg of CuBr (0.06 mmol) was added to the solution, which became dark brown. After another freeze-pump-thaw cycle, the reaction was allowed to proceed at room temperature for 12 hours. To quench the reaction, the Schlenk flask was exposed to air, and the solution turned blue. The mixture was transferred to a 50-mL centrifuge tube and washed with an EDTA•2Na saturated solution 3 times until no blue color was observed, deionized water 8-12 times, and acetone twice. In each step the polymer-grafted silica particle was recollected via centrifugation. The product was dried in vacuum at 60 °C overnight. After drying, TGA was performed to determine the extent of polymer grafting.

Surface-initiated ATRP of silica-copolymer-2 (silica-poly(PEGMA-1100-*co*-PEGMA-300), 1:1), silica-copolymer-3 (silica-poly(PEGMA-1100-*co*-PEGMA-475), 1:1), silica-copolymer-4 (silica-poly(PEGMA-300-*co*-PEGMA-475), 1:1), silica-copolymer-5 (silica-poly(PEGMA-1100-*co*-PEGMA-232), 3:7), silica-copolymer-6 (silica-poly(PEGMA-1100-*co*-PEGMA-300), 3:7), silica-copolymer-7 (silica-poly(PEGMA-1100-*co*-PEGMA-475), 3:7), silica-copolymer-8 (silica-poly(PEGMA-300-*co*-PEGMA-475), 3:7), silica-copolymer-9 (silica-poly(PEGMA-300-*co*-PEGMA-475), 7:3) were conducted following the same protocol with the specified monomer ratios.

In all cases the total amount of monomer in solution was 1 mmol. Fig. 2 and Table 2 describe TGA profiles and weight loss.

2.6 ATRP of free poly(PEGMA) homopolymers and copolymers in solution

ATRP of free tri(ethylene glycol) methyl ether methacrylate (poly(PEGMA-232)) in solution. The monomer was dissolved in methanol and passed through an activated basic alumina column to remove inhibitor. After removing solvent, 1160 mg of tri(ethylene glycol) methyl ether methacrylate (5 mmol), 19.5 mg of ethyl 2-bromoisobutyrate (0.1 mmol, EBiB), and 62.5 mg of 2, 2'-bipyridine (bpy, 0.4 mmol) were dissolved in 1 mL of deionized water and 3 mL of methanol in a Schlenk flask. The mixture was ultrasonicated for 15-20 minutes. After 3 freeze-pump-thaw cycles, the Schlenk flask was filled with nitrogen, 28.7 mg of CuBr (0.2 mmol) was added, and the solution immediately turned brown. After another freeze-pump-thaw cycle, the reaction was allowed to proceed at room temperature for 12 hours. To quench the reaction, the Schlenk flask was exposed to air, after which the solution turned blue. The mixture was diluted in deionized water and passed through an activated basic alumina column to remove copper catalyst. After removing solvent, the polymer was dried under vacuum (≤ 10 mTorr) for 24 hours at 70 °C. Since no vinyl proton signal was observed in the ^1H NMR spectrum, indicating all monomers were consumed during polymerization, the reaction conversion should be $\geq 99\%$. The polymer (1.037 g, 89% yield) obtained was a colorless, highly viscous liquid.

ATRP of poly(PEGMA-188), poly(PEGMA-300), poly(PEGMA-475), and poly(PEGMA-1100) free polymers followed the same protocol using the same number of moles of monomer in each case.

ATRP of free copolymer-1 (poly(PEGMA-1100-*co*-PEGMA-232), 1:1), copolymer-2 (poly(PEGMA-1100-*co*-PEGMA-300), 1:1), copolymer-3 (poly(PEGMA-1100-*co*-PEGMA-475), 1:1), copolymer-4 (poly(PEGMA-300-*co*-PEGMA-475), 1:1), copolymer-5 (poly(PEGMA-1100-*co*-PEGMA-232), 3:7), copolymer-6 (poly(PEGMA-1100-*co*-PEGMA-300), 3:7), copolymer-7 (poly(PEGMA-1100-*co*-PEGMA-475), 3:7), copolymer-8 (poly(PEGMA-1100-*co*-PEGMA-475), 3:7), copolymer-9 (poly(PEGMA-300-*co*-PEGMA-475), 7:3) were conducted following the same protocol with different copolymerization ratio calculated. The total amount of monomer employed in all cases was 1 mmol.

2.7 Preparation of hybrid silica/polymer and free polymer electrolytes

Hybrid silica-poly(PEGMA) nanocomposite electrolyte preparation. Hybrid electrolytes were prepared by dissolving LiI and I₂ (10:1 mole ratio) in the host poly(ethylene glycol) dimethyl ether (PEGDME-500, M_n = 500) electrolyte, and then dispersing PEGMA/silica nanoparticles in this PEGDME. The mole ratio of PEGDME-500/LiI/I₂ was fixed at 100:10:1. Since the number of ethylene oxide (EO) repeating units in PEGDME-500 is around 10, the EO to Li ratio is 100:1 in the PEGDME-500/LiI/I₂ mixture. Specifically, 78 mg of I₂ (0.3 mmol) and 403.7 mg of LiI (3 mmol) were mixed into 15 g of PEGDME-500 (30 mmol) in a vial. The vial was sealed with parafilm, covered with aluminum foil, and the electrolyte was stirred overnight until the salt species dissolved. A clear, dark orange/brown liquid resulted. In this electrolyte, every 258 mg of liquid contained 5 mmol PEO (50 mmol EO), 0.5 mmol LiI, and 0.005 mmol I₂ (PEGDME-500/LiI/I₂ = 100/10/1). When dispersing nanoparticles in this electrolyte, to guarantee the same EO/Li ratio for all hybrid electrolytes, the mole ratio of PEGMA EO

to the previously added lithium salt was fixed at 10:1 during each particle addition. Therefore, when including ethylene oxide units in both PEGDME-500 and silica-poly(PEGMA), the total EO/Li ratio was 110:1 for all hybrid electrolytes. The amount of poly(PEGMA)-coated silica to add to the electrolyte was calculated according to TGA data and molecular weight (for the copolymers, we assumed that the ratio of monomers incorporated into the polymer was the same as that in solution). Therefore, to make hybrid electrolyte, in every 258 mg of freshly prepared PEGDME-500/Li/I₂ electrolyte, the following amount of hybrid particles were added (0.5 mmol EO from silica-poly(PEGMA) were added in all cases): 57.1 mg silica-poly(PEGMA-188), 43.1 mg silica-poly(PEGMA-232), 33.1 mg silica-poly(PEGMA-300), 29.4 mg silica-poly(PEGMA-475), 26.5 mg silica-poly(PEGMA-1100), 31.3 mg silica-poly(PEGMA-1100-*co*-PEGMA-232) (1:1), 28.6 mg silica-poly(PEGMA-1100-*co*-PEGMA-300) (1:1), 29.9 mg silica-poly(PEGMA-1100-*co*-PEGMA-475) (1:1), 31.4 mg silica-poly(PEGMA-300-*co*-PEGMA-475), 32.4 mg silica-poly(PEGMA-1100-*co*-PEGMA-232) (3:7), 29.1 mg silica-poly(PEGMA-1100-*co*-PEGMA-300) (3:7), 30.5 mg silica-poly(PEGMA-1100-*co*-PEGMA-475) (3:7), 30.3 mg silica-poly(PEGMA-300-*co*-PEGMA-475) (3:7), 31.5 mg silica-poly(PEGMA-300-*co*-PEGMA-475) (7:3). Electrolytes containing silica-poly(PEGMA-1100) were particularly viscous and solidified easily. A Wig-L-Bug was used to homogenize these particles in the PEGDME-500/Li/I₂ electrolyte, while the other samples were stirred for 24 hours with a magnetic stirring bar in a parafilm-sealed, aluminum-covered vial. For a control experiment, a set of electrolytes containing PEGDME-500/Li/I₂ with no particles but having the same EO/Li ratio was also prepared

by adding 25 mg PEGDME-500 into 258 mg of previously prepared PEGDME-500/LiI/I₂ electrolyte.

Poly(PEGMA) free polymer electrolyte preparation. The mole ratio of PEGDME-500/LiI/I₂ was again fixed at 100:10:1, with EO:Li = 100:1 in the mixture. While dispersing free polymers into the system, the mole ratio of PEGMA EO to lithium salt was fixed at 10:1. Therefore, when including EO units in both PEGDME-500 and free poly(PEGMA), the total EO/Li ratio was fixed at 110:1 in all electrolytes. The amount of free poly(PEGMA) was calculated according to molecular weight. For every 258 mg of PEGDME-500/LiI/I₂ electrolyte, the following amounts of free polymers were added (0.5 mmol of EO in poly(PEGMA) in all cases): 38.8 mg poly(PEGMA-232), 29.9 mg poly(PEGMA-300), 26.5 mg poly(PEGMA-475), 23.9 mg poly(PEGMA-1100), 25.6 mg poly(PEGMA-1100-*co*-PEGMA-232) (1:1), 25.0 mg poly(PEGMA-1100-*co*-PEGMA-300) (1:1), 24.6 mg poly(PEGMA-1100-*co*-PEGMA-475) (1:1), 27.7 mg poly(PEGMA-300-*co*-PEGMA-475) (1:1), 27.4 mg poly(PEGMA-1100-*co*-PEGMA-232) (3:7), 26.0 mg poly(PEGMA-1100-*co*-PEGMA-300) (3:7), 25.1 mg poly(PEGMA-1100-*co*-PEGMA-475) (3:7), 27.0 mg poly(PEGMA-300-*co*-PEGMA-475) (3:7), 28.4 mg poly(PEGMA-300-*co*-PEGMA-475) (7:3). All these electrolytes were dark brown, viscous liquids.

2.8 Ionic conductivity measurements

Temperature-dependent ionic conductivity measurements were determined from electrical impedance analysis (EIS) using a homemade cell. The data were obtained with a Hewlett-Packard 4192A LF Impedance Analyzer over a frequency range of 5 Hz to 13 MHz with an applied oscillating voltage of 10 mV. The sample cell uses two steel disks

as symmetrical electrodes separated by a 0.02 cm-thick sample in a Teflon collar. The sample radius is 0.6 cm. All electrolytes were pipetted into the cell, and impedance measurements were obtained at 5 °C intervals from 25 – 90 °C. The sample was equilibrated at the pre-determined temperature for 15 minutes before each measurement. Ionic conductivity was calculated:

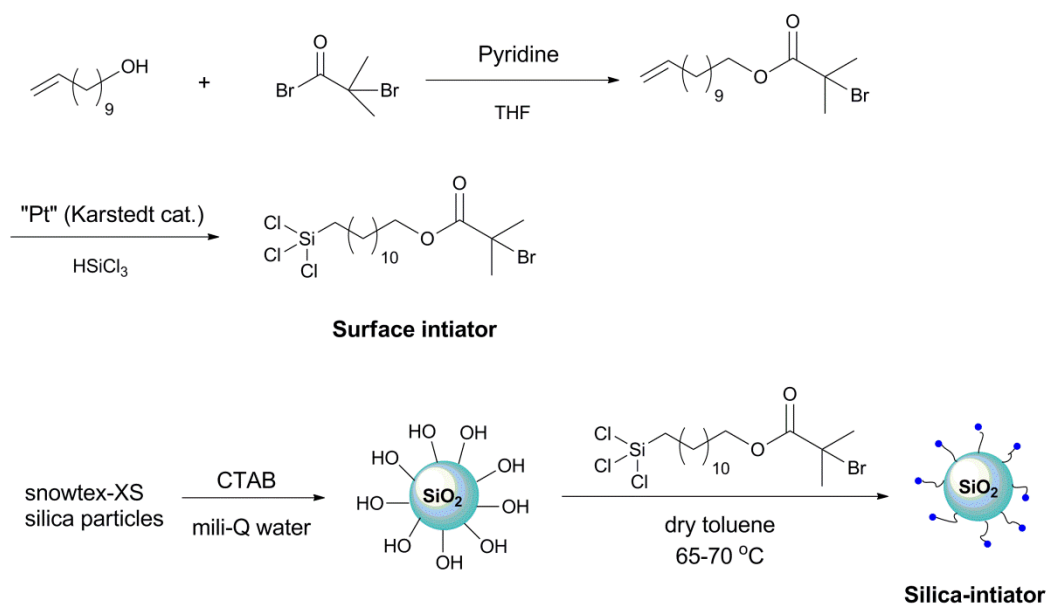
$$\sigma = l/\rho = l/(R \cdot A)$$

where l (cm) refers to the measured distance and A (cm²) is the cross-sectional area. To avoid moisture, all samples were dried under vacuum (≤ 10 mTorr) at 70 °C for at least 48 hours. All conductivity measurements were conducted in the glove box.

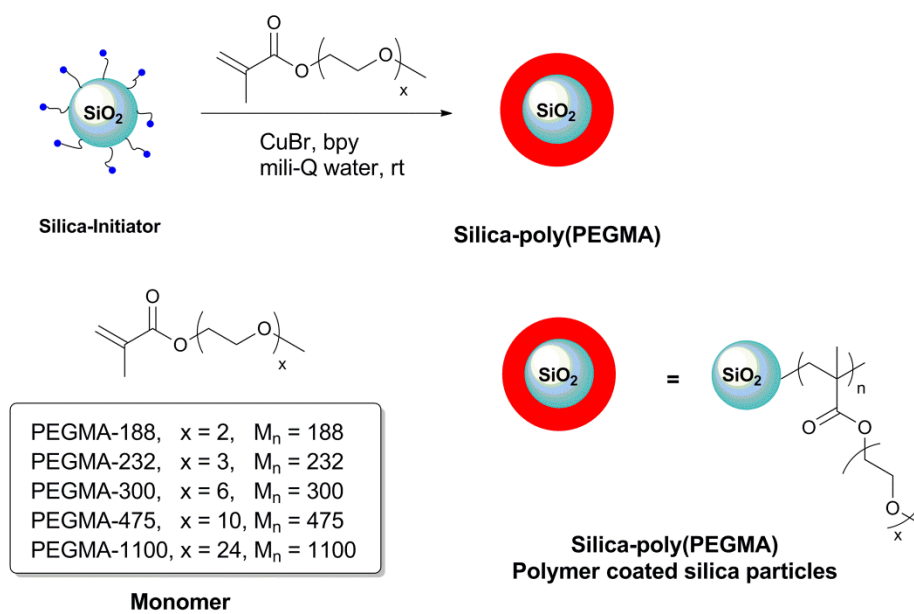
3 Results and discussion

3.1 Synthesis of silica-poly(PEGMA) nanoparticles

The first step in growing polymers from silica nanoparticles is attachment of an ATRP initiator to the surface via silanization (Scheme 2). Synthesis of the silane-containing surface initiator, (11-(2-bromo-2-methyl) propionyloxy)undecyl-trichlorosilane, proceeded in two steps according to a literature procedure.⁴¹ The initiator was then anchored onto silica surface via silane chemistry. Subsequent surface-initiated ATRP (Scheme 3) of poly(ethylene glycol) methyl ether methacrylate (PEGMA) (Table 1) gave the modified particles. Variation of the length of the PEG chain in PEGMA should allow tailoring of particle properties.



Scheme 2 Synthesis of a silane-containing ATRP initiator, and attachment of this initiator to silica nanoparticles



Scheme 3 Surface-initiated ATRP of PEGMA homopolymer from silica-initiator nanoparticles to form silica-poly(PEGMA)

Table 1 Silica-poly(PEGMA) synthesized in this work

Silica-Polymer	Monomer	x ^a
Silica-poly(PEGMA-188)	PEGMA-188, M _n =188	2
Silica-poly(PEGMA-232)	PEGMA-232, M _n =232	3
Silica-poly(PEGMA-300)	PEGMA-300, M _n =300	6
Silica-poly(PEGMA-475)	PEGMA-475, M _n =475	10
Silica-poly(PEGMA-1100)	PEGMA-1100, M _n =1100	25

^a x refers to an estimation of the number of ethylene oxide repeating units in the monomer, as derived from the average molecular weight given by the manufacturers.

FT-IR spectroscopy confirms the polymer grafting. The FT-IR spectrum (Fig. 1) of bare silica nanoparticles shows a characteristic broad absorption band associated with Si-O-Si stretching (1100 cm^{-1}), and a sharp band at around $800\text{-}770\text{ cm}^{-1}$ corresponding to Si-OH stretching. The C-H stretching band at $3000\text{-}2800\text{ cm}^{-1}$ likely stems from residual CTAB. The abundant broad band at $3600\text{-}3200\text{ cm}^{-1}$ (Fig. 1a) is due to the hydroxyl groups on the silica surface, which are partly consumed after reaction with the initiator (11-(2-bromo-2-methyl)propionyloxy) undecyltrichlorosilane. After surface-initiated ATRP, the ester carbonyl stretch of the methacrylate appears between 1750 and 1700 cm^{-1} . Another characteristic peak associated with the C-O-C stretching of PEO is present between 1300 and 1100 cm^{-1} . This absorbance along with C-H stretching modes ($3000 - 2800\text{ cm}^{-1}$) become less intense with increasing length of the PEO side chain.

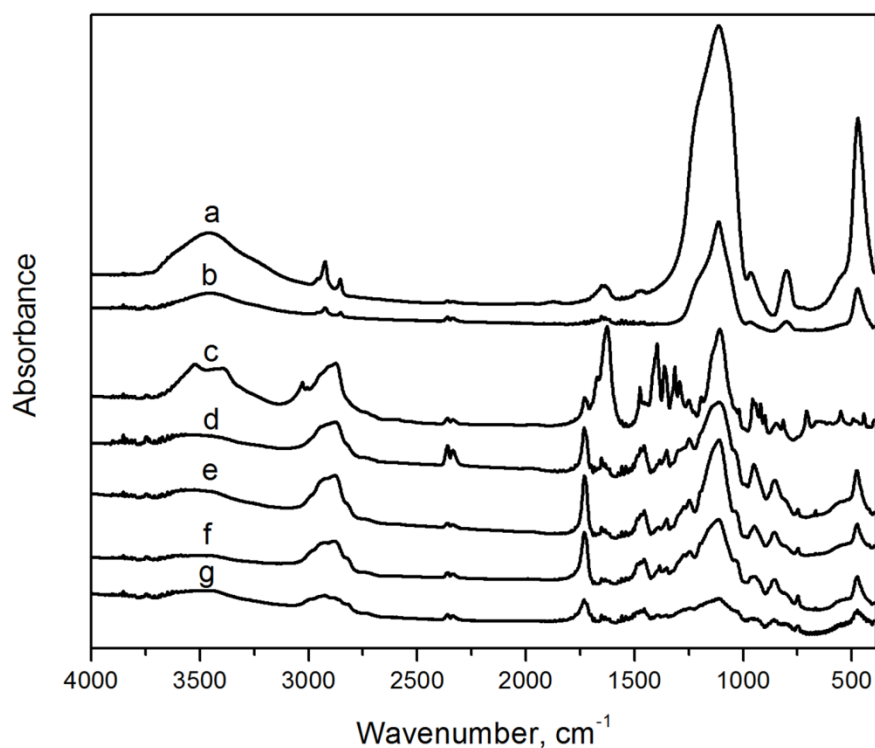


Fig. 1 FT-IR spectra of (a) bare silica particles, (b) silica-initiator nanoparticles, (c) silica-poly(PEGMA-1100) nanoparticles, (d) silica-poly(PEGMA-475) nanoparticles, (e) silica-poly(PEGMA-300) nanoparticles, (f) silica-poly(PEGMA-232) nanoparticles, and (g) silica-poly(PEGMA-188) nanoparticles

The polymer grafted nanoparticles are also confirmed through TEM (Fig. S1). Bare silica particles precipitated by CTAB show diameters around 16 nm, which is about three times the diameter given by the manufacture. This may reflect some particle aggregation during the extensive wash/centrifugation/redispersion process to remove excess surfactant. After initiator attachment, aggregation became more severe even with ultrasonication during sample preparation. TEM clearly shows the aggregation (Fig. S1b).

This is presumably due to the long PEO-containing polymer side chains were tangled together make them hard to isolate into well-dispersed single particle. Moreover, Fig. S1c shows that after surface-initiated polymerization, silica-poly(PEGMA) particles can aggregate into a 100-nm particles. The dark spots in Fig. S1c are the silica cores, while the abundant gray area between these cores is the poly(PEGMA) shells. The TEM image suggests significant polymer grafting from the silica surface, and thermogravimetric analysis was performed to quantitatively determine the amount of organic content.

3.2 Thermal properties of silica-poly(PEGMA) nanocomposites

Thermogravimetric analysis (TGA) allows estimation of the extent of surface-initiated polymerization. TGA occurred in air with temperatures ramped to 850 °C. Under the presence of oxygen at this high temperature, the organic portion (i.e. polymer and initiator) of the modified particles completely decompose and vaporizes with air flow, to leave behind an inorganic silica core. Therefore, weight loss quantitatively reveals the amount of polymer grafted on silica particles. Table 2 and experimental section examine the extent of polymer growth in more detail.

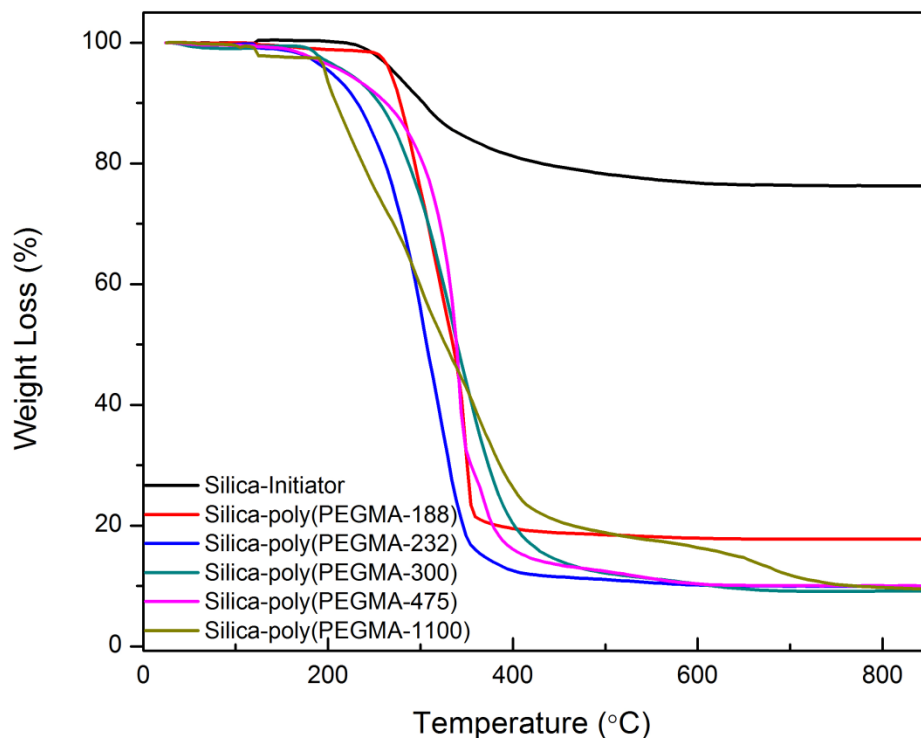


Fig. 2 TGA data for silica-initiator and silica-poly(PEGMA) nanoparticles

Table 2 DSC and TGA result for silica-poly(PEGMA)

Silica-poly(PEGMA)	T_g (°C) ^a	T_m (°C) ^a	Weight loss ^b	Maximum weight loss ^c
Silica-poly(PEGMA-188)	-49.4	n/a	82.2%	88.2%
Silica-poly(PEGMA-232)	-61.6	n/a	89.2%	90.2%
Silica-poly(PEGMA-300)	-62.4	n/a	90.8%	92.2%
Silica-poly(PEGMA-475)	-70.5	-7.3	89.9%	95.7%
Silica-poly(PEGMA-1100)	n/a	35.7	90.3%	97.7%

^a T_g and T_m of silica-polymer nanoparticles were determined from DSC data. ^b % of weight loss was obtained from TGA. Materials were heated up to 850°C under air. ^c

Maximum weight loss is the theoretical weight loss calculated from monomer to initiator ratio during polymerization. The calculation details are in experimental section.

The T_g of pure PEO ranges from -60 to -30 °C, depending on the number of repeating ethylene oxide (EO) units. Additionally, when the number of EO repeating units is > 8 , PEO tends to crystallize,⁴³ choosing its most stable conformation—the 7_2 helix.⁴⁴ Upon crystallization, the polymer chain becomes rigid, and hence the conductivity of PEO-based electrolyte decreases. DSC data (Fig. 3) show that with shorter PEO side chains (e.g. silica-poly(PEGMA-188), silica-poly(PEGMA-232), and silica-poly(PEGMA-300)), no crystallization occurs so a melting temperature is not observed over the operation range. However, for silica-poly(PEGMA-475) and silica-poly(PEGMA-1100), especially the latter, a sharp and strong endothermic peak due to crystallization appears in the DSC curve. Fig. 3 and Table 2 show that the value of T_g decreases with the length of the PEO side chain, and the T_g of silica-poly(PEGMA-1100) is below the range of our instrument (≥ -85 °C). Below T_g , the polymer is a glass where chains show regions of three-dimensional order, but after passing through glass transition, the polymer softens and becomes rubber like. The T_g correlates with the flexibility of the polymer chains, and greater flexibility should enhance ion conductivity.

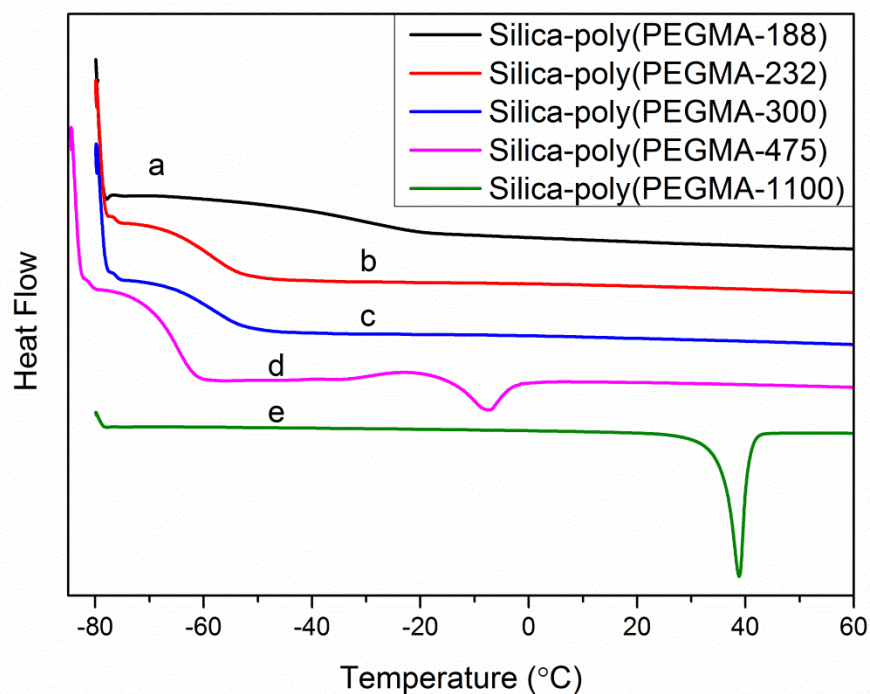


Fig. 3 DSC results of (a) silica-poly(PEGMA-188); (b) silica-poly(PEGMA-232); (c) silica-poly(PEGMA-300); (d) silica-poly(PEGMA-475) and (e) silica-poly(PEGMA-1100)

3.3 Ionic conductivity of electrolytes containing PEO mixed with silica-poly(PEGMA) nanoparticles

Hybrid electrolytes were prepared by dissolving LiI and I₂ (10:1 mole ratio) in poly(ethylene glycol) dimethyl ether (PEGDME-500, M_n = 500), with the mole ratio of PEGDME-500/LiI/I₂ fixed at 100:10:1 (EO to Li ratio of ~ 100:1, PEGDME-500 contains around 10 EO units), and subsequently dispersing the silica-poly(PEGMA) nanoparticles into the mixture. The amount of coated nanoparticles added was calculated from TGA data (see experimental section for details) to achieve a total EO:Li ratio in the

electrolyte (including EO from PEGDME and silica-poly(PEGMA) of approximately 110:1. Control experiments employed a set of electrolytes consisting of PEGDME-500/LiI/I₂ with no particles but an EO/Li ratio of 110:1. Fig. 4 shows that vigorous stirring of functionalized particles in the PEGDME/LiI/I₂ mixture for at least 24 hours resulted in homogeneous electrolytes. For very viscous samples, such as silica-poly(PEGMA-1100), agitation with a Wig-L-Bug facilitated formation of a homogeneous hybrid electrolyte. Upon the introduction of particles, the electrolyte gelled, and with an increasing length of PEO side chains, the viscosity of the electrolyte increased dramatically. Electrolytes containing silica-poly(PEGMA-475) and silica-poly(PEGMA-1100) did not flow.

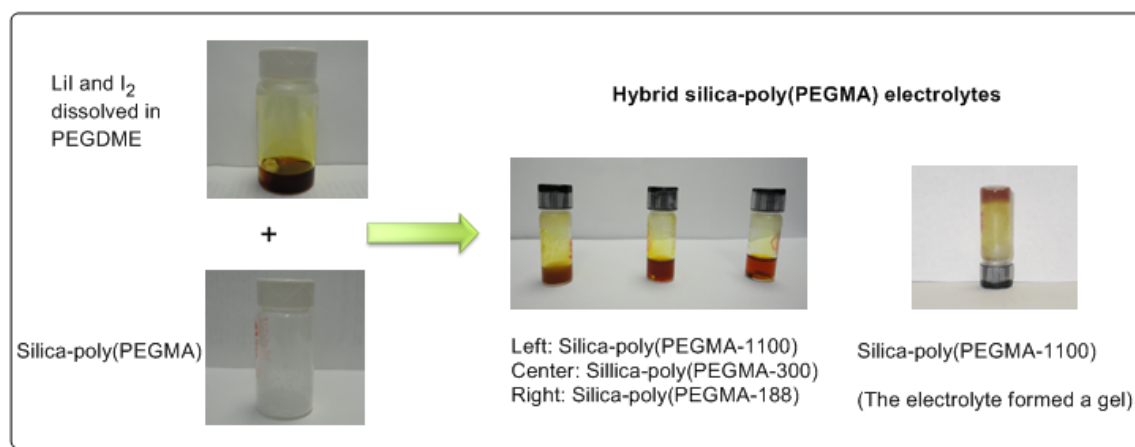


Fig. 4 Photographs showing electrolytes formed by dispersing silica-poly(PEGMA) in PEGDME containing LiI and I₂

Using electrochemical impedance spectroscopy (EIS), we determined the conductivity of the hybrid polymer electrolytes. Fig. 5 shows conductivity values at temperature ranging from 20 °C to 90 °C with 5 °C intervals, plotted versus 1000/T. The

slight convex curvatures of hybrid silica-poly(PEGMA) electrolytes plots indicates a typical VFT model of ion conduction mechanism.⁴⁵ As expected, the ionic conductivity increased with temperature because of enhanced chain mobility. Room-temperature conductivities of all electrolytes containing silica-poly(PEGMA) range from 6×10^{-5} to 1.2×10^{-4} S/cm. Despite its solidification, the electrolyte with silica-poly(PEGMA-1100) shows higher ionic conductivity than other electrolytes with modified silica particles. As discussed previously, three parameters control ionic conductivity: the charge carrier (ion) concentration (n), ion charge (q), and ion mobility (μ). The amount of silica-poly(PEGMA) particles added into PEGDME/LiI/I₂ gave the same EO/Li ratio in all electrolytes, and the silica cores occupy only a small part of the volume because over 90% of the nanoparticle mass is polymer. Hence, the charge carrier concentration for all electrolyte samples should be similar. Because ion transport in the polymer matrix depends on the segmental movement of the polymer chain in the amorphous phase, and lithium ion coordinates to 4 – 8 oxygen atoms, the relatively high conductivity of silica-poly(PEGMA-1100) has two possible explanations: a lower T_g (i.e. higher chain mobility); or lithium coordination with more oxygen atoms.⁴⁶ To further study the Li—oxygen coordination, the equivalent weight (EW) value of EO functional group in silica-poly(PEGMA) particles were calculated from TGA data (Table 2). The calculation was shown in Table S1. As concluded from the table, the EW values of EO functional group in silica-poly(PEGMA) nanoparticles increase with the increase of the PEO side chain. Therefore, with shorter PEO side chains, lithium coordination to fewer oxygen atoms might allow formation of Li cation, which will decrease ionic conductivity.

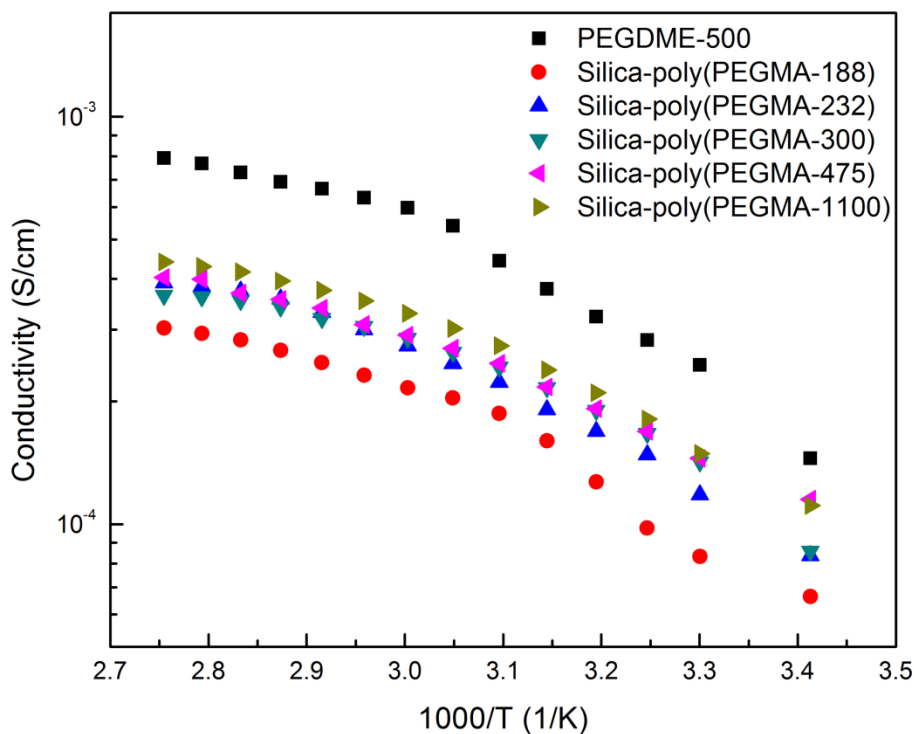


Fig. 5 Temperature dependent ionic conductivities of electrolytes formed by dispersing silica-poly(PEGMA) in PEGDME containing LiI and I₂ (The figure also shows data for PEGDME/LiI/I₂ without the modified particles.)

3.4 Copolymerization to form silica-poly(PEGMA) nanocomposites

Since ion transport only takes place in the amorphous phase, crystallization of long PEO side chains should decrease conductivity.²¹ Even though silica-poly(PEGMA-475) and silica-poly(PEGMA-1100) show relatively high ionic conductivity, partial crystallization of PEO side chains might hinder the ion transport in the polymer matrix. Crystallization should be especially detrimental for silica-poly(PEGMA-1100), which has a T_m value around 35 °C. Consequently, decreasing the degree of crystallinity and thus

Table 3 DSC and TGA data for silica nanoparticles modified with grafted PEGMA copolymers

Silica-copolymer	Monomers		T _g (°C) ^a	T _m (°C) ^a	Weight loss ^b	Maximum weight loss ^c
	A	B				
Silica-copolymer-1	PEGMA-1100 (50%)	PEGMA-232 (50%)	/	38.8	81.9%	96.3%
Silica-copolymer-2	PEGMA-1100 (50%)	PEGMA-300 (50%)	-66.8	21.7	87.5%	96.4%
Silica-copolymer-3	PEGMA-1100 (50%)	PEGMA-475 (50%)	-67.6	18.8	82.2%	96.8%
Silica-copolymer-4	PEGMA-300 (50%)	PEGMA-475 (50%)	-64.9	/	88.2%	93.8%
Silica-copolymer-5	PEGMA-1100 (30%)	PEGMA-232 (70%)	-65.6	23.1	84.8%	90.7%
Silica-copolymer-6	PEGMA-1100 (30%)	PEGMA-300 (70%)	-65.5	8.6	88.8%	90.7%
Silica-copolymer-7	PEGMA-1100 (30%)	PEGMA-475 (70%)	-67.3	19.5	82.5%	92.8%
Silica-copolymer-8	PEGMA-300 (30%)	PEGMA-475 (70%)	-65.3	/	88.2%	89.3%
Silica-copolymer-9	PEGMA-300 (70%)	PEGMA-475 (30%)	-62.2	/	86.1%	87.5%

^a: T_g and T_m of silica/polymer nanoparticles were obtained from DSC data. ^b: % weight loss was determined from TGA. Materials were heated to 850°C in air. ^c: Maximum weight loss is the theoretical weight loss calculated from the monomer to initiator ratio.

Silica-copolymers exhibit TGA profiles similar to those of silica-homopolymers (compare Fig. S2 and Fig. 2). The onset decomposition temperatures of the silica-copolymers are above 200 °C and in some cases as high as 400 °C. The formation of copolymers containing PEGMA-1100 and monomers with shorter PEO side chains hinders the crystallization of poly(PEGMA-1100). Table 3 shows decreased T_m values for the copolymers in most cases (Table 2 shows that the T_m value for the

silica-poly(PEGMA-1100) homopolymer is 36°C). Among the copolymers, silica-copolymer-6, with PEGMA-1100 and PEGMA-300 in a 3:7 ratio, shows melting at below room temperature (8.6 °C). Because PEO is predominantly in the amorphous phase above its melting point, we expect the room-temperature ionic conductivity of hybrid silica-copolymer-6 electrolyte to exceed the conductivity of the silica-poly(PEGMA-1100) electrolyte. To examine this hypothesis, we prepared hybrid silica-copolymer electrolytes with the protocol discussed previously and determined ionic conductivity as a function of temperature.

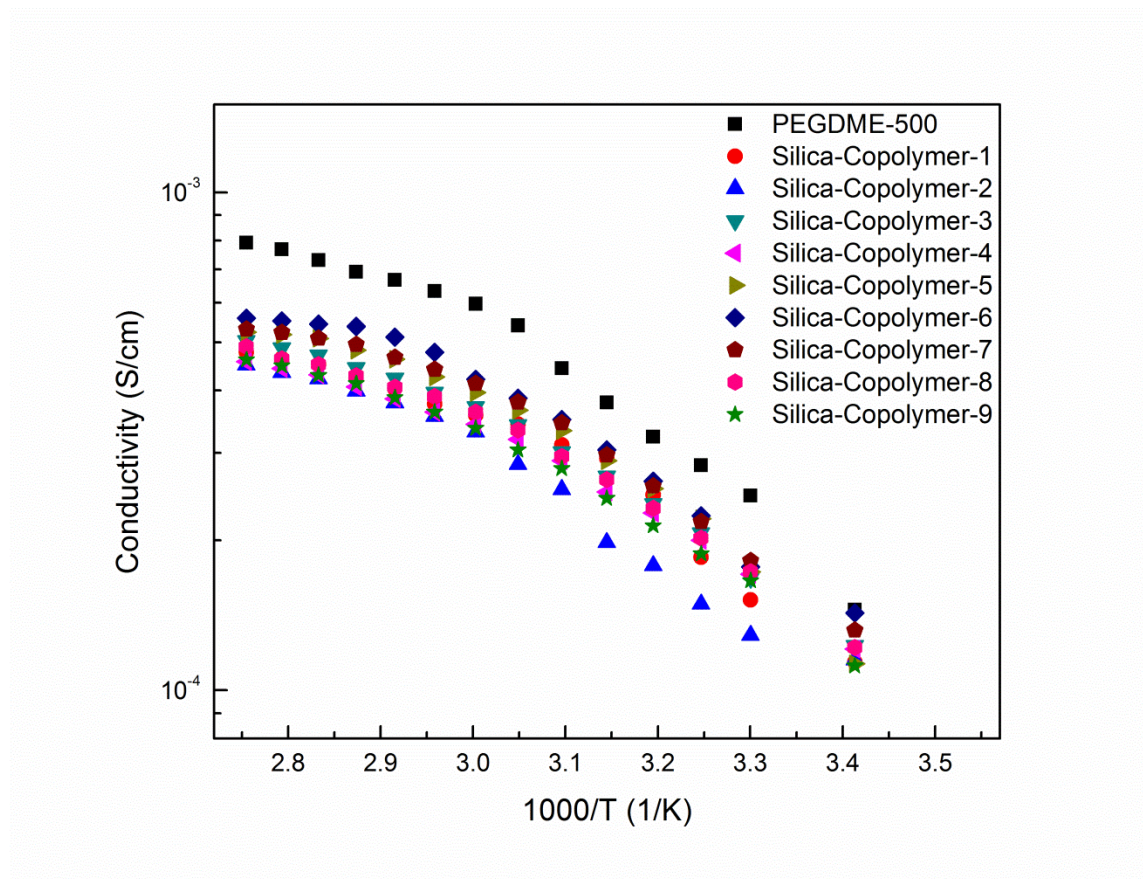


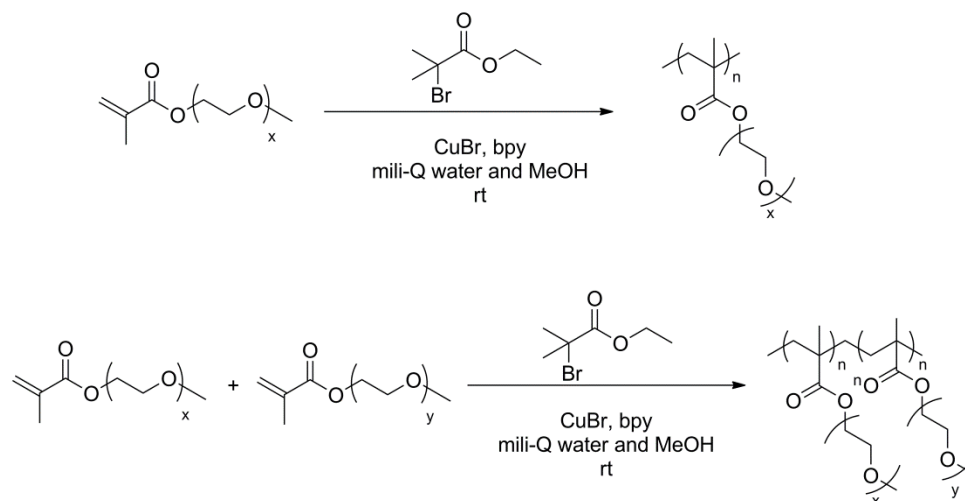
Fig. 6 Temperature dependent ionic conductivities of electrolytes formed by silica-poly(PEGMA) copolymers in PEGMDE containing LiI/I_2 . The figure also shows data for PEGDME/ LiI/I_2 without modified particles.

Fig. 6 presents the temperature-dependent ionic conductivity of electrolytes containing silica-poly(PEGMA) copolymers. These plots for electrolytes containing silica-copolymer also exhibit the VFT behavior, showing excellent fits with VFT equation, which suggests ion transport is highly coupled with segmental movement of polymer chain. Room temperature ionic conductivities for hybrid silica-copolymer electrolytes ranged from 1.1×10^{-4} to 1.5×10^{-4} S/cm, which is approximately two to three times higher than the conductivity of either corresponding electrolyte with silica-

poly(PEGMA) homopolymers, even though the highest ionic conductivity was still less than one order of magnitude lower than the reference (PEGDME-500 electrolyte) conductivity. As Table 3 reveals, silica-copolymer-6, which exhibits the lowest melting point among copolymers with PEGMA-1100 as one of the monomers, gives the highest electrochemical conductivity, which is also higher than the silica-poly(PEGMA-1100) homopolymer electrolyte. In addition, PEGMA copolymer coated particles are excellent gelators. The polymer electrolytes became very viscous with the introduction of the particles. In particular, silica-poly(PEGMA-1100-*co*-PEGMA-300) and silica-poly(PEGMA-1100-*co*-PEGMA-475) solidified easily after mixing with PEGDME/LiI/I₂ and yet, gave reasonably high ionic conductivity.

3.5 Synthesis and characterization of free poly(PEGMA) electrolytes

To compare the performance of polymer coated hybrid electrolytes with the corresponding free PEGMA homopolymers and copolymers, we synthesized a series of free polymers (Scheme 5). All structures were confirmed by ¹H NMR. Fig. 7 gives the NMR spectrum of poly(PEGMA-232) as an example.



Scheme 5 ATRP of free poly(PEGMA) homopolymers (top) and free poly(PEGMA) copolymers (bottom)

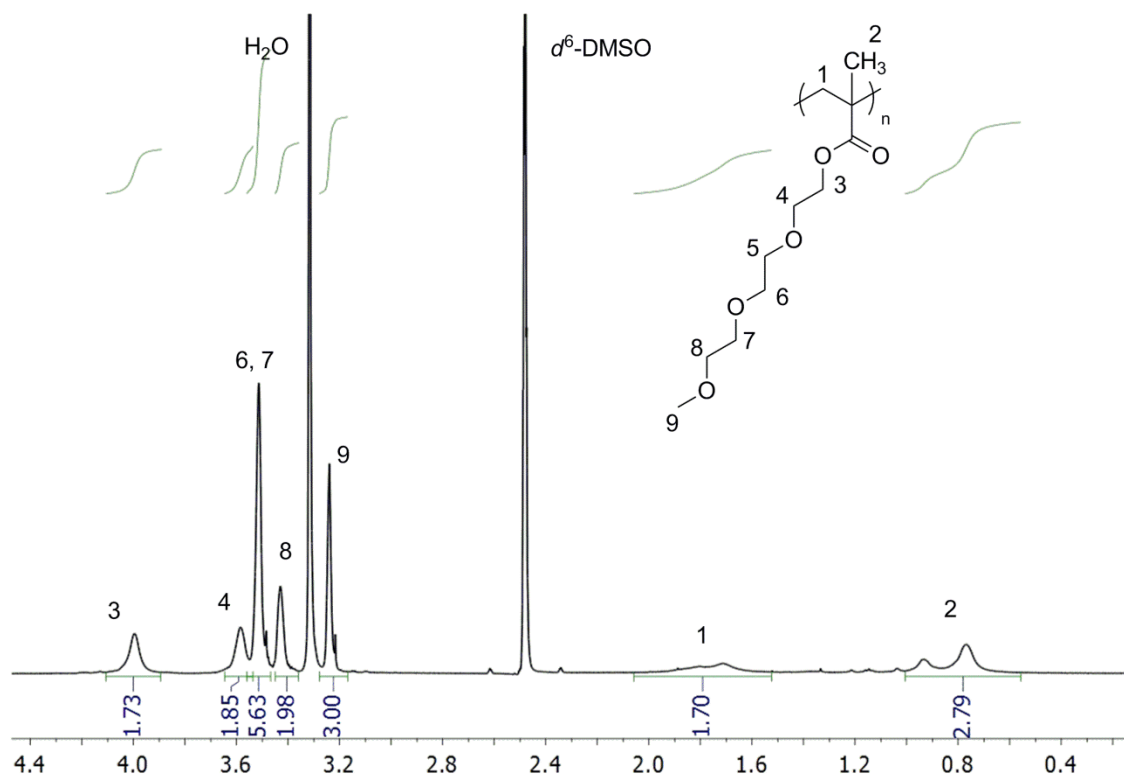


Fig. 7 NMR spectrum of free poly(PEGMA-232)

FT-IR spectra of free poly(PEGMA) (Fig. S3) further confirm polymer structure. Free polymer electrolytes were prepared via the same protocol for silica-poly(PEGMA) electrolytes. Fig. 8 shows conductivities of free poly(PEGMA) electrolytes containing LiI/I₂ dissolved in PEGDME, with the same EO/Li ratio as for electrolytes with poly(PEGMA)-coated silica. Like hybrid silica-polymer electrolytes, the plots of electrolytes containing free poly(PEGMA) show good fits to the VFT equation, suggesting the same ion hopping mechanism in both systems. Room-temperature ionic conductivities for free polymer electrolytes ranged from 1.2×10^{-4} to 1.5×10^{-4} S/cm, essentially the same values determined for corresponding hybrid electrolytes. Therefore, compared to the conductivity of free poly(PEGMA) electrolyte with the same EO/Li ratio, immobilizing poly(PEGMA) on silica particles has a negligible effect on ionic conductivity. However, immobilization of the poly(PEGMA) on silica leads to solid electrolytes that should be much more amenable to encapsulation in devices.

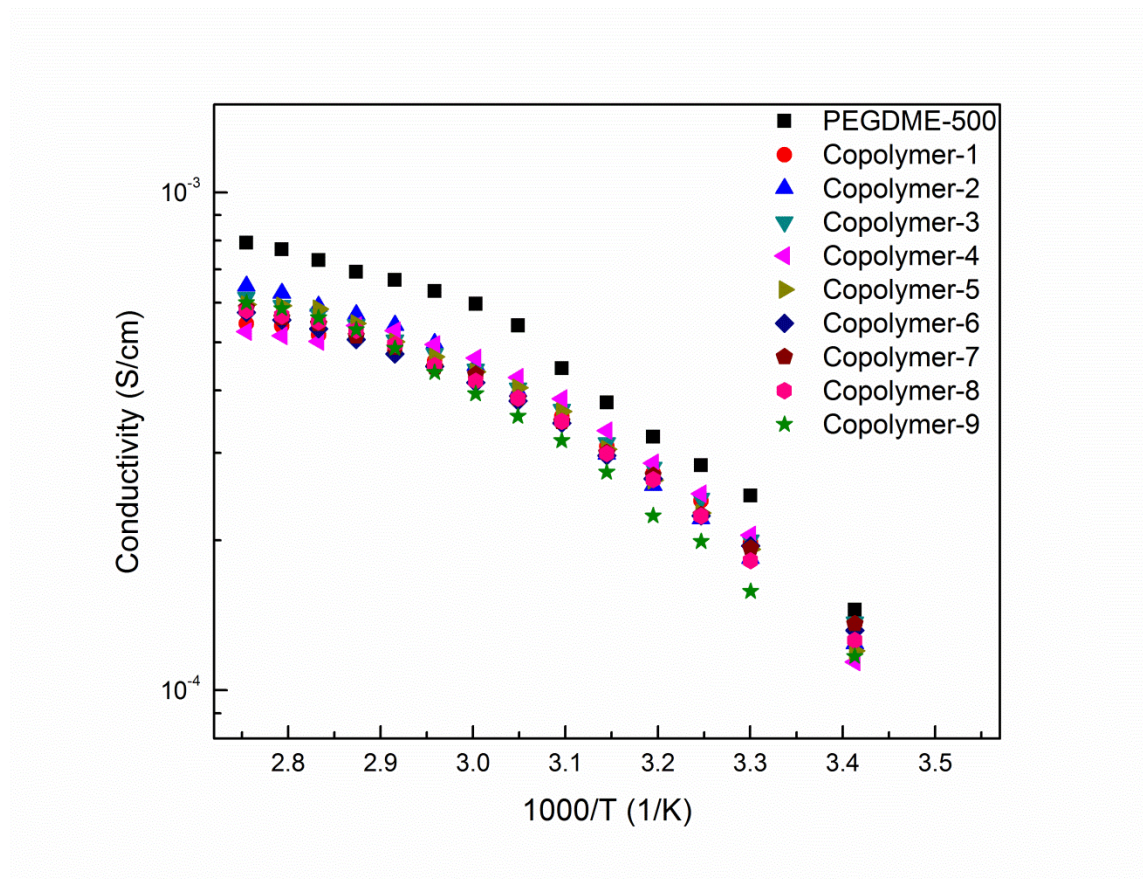


Fig. 8 Temperature-dependent ionic conductivities of electrolytes formed by free poly(PEGMA) copolymers in PEGDME containing LiI/I₂. The figure also shows data for PEGDME/ LiI/I₂ without modified particles.

4 Conclusions

To summarize, hybrid silica/polymer nanocomposites were synthesized by grafting various PEGMA based polymers onto silica nanoparticles via surface-initiated ATRP. Polymer electrolytes were prepared by blending silica-poly(PEGMA) particles with PEGDME-500 containing LiI/I₂ to create potential candidates for electrolytes in DSSCs. The introduction of silica nanoparticles enhanced the electrolyte mechanical properties, making the electrolytes viscous gels. These solid-like polymer/inorganic

hybrid electrolytes still show room temperature conductivity around 10^{-4} S/cm, only a 3-fold decrease compared to an electrolyte with only PEGDME-500 and LiI/I₂. Copolymerization of two PEGMA monomers circumvents the problem of PEO crystallization because a short PEO side chain interrupts the structure of the longer side chain. This lack of crystallization, however, only increases conductivity by a factor of two when comparing electrolytes containing nanoparticles modified with homo and copolymers. Conductivities of PEGDME-500/LiI/I₂ containing silica-copolymer electrolytes and corresponding free copolymers are nearly identical. However, the silica-copolymer electrolytes are highly viscous gels that are much more amenable to encapsulation. Our ongoing research will focus on utilizing these novel electrolytes in DSSCs or LIBs.

ACKNOWLEDGMENTS

We thank the National Science Foundation (DMR-0934568) for funding this research and MSU Composite Materials and Structures Center (CMSC). Z. Jia thanks Dr. James Jackson, Dr. Milton Smith, and Dr. Merlin Bruening for valuable discussion.

Notes and references

1. Z. Ning, Y. Fu and H. Tian, *Energy & Environmental Science*, 2010, 3, 1170.
2. A. Hagfeldt, G. Boschloo, L. Sun, L. Kloo and H. Pettersson, *Chemical Reviews*, 2010, 110, 6595-6663.
3. B. O'Regan and M. Grätzel, *Nature*, 1991, 353, 737-740.
4. M. Grätzel, *Accounts of Chemical Research*, 2009, 42, 1788-1798.
5. J. Halme, P. Vahermaa, K. Miettunen and P. Lund, *Advanced materials*, 2010, 22, E210-234.
6. M. Armand and J. M. Tarascon, *Nature*, 2008, 451, 652-657.
7. P. G. Bruce, B. Scrosati and J.-M. Tarascon, *Angewandte Chemie International Edition*, 2008, 47, 2930-2946.
8. J. M. Tarascon and M. Armand, *Nature*, 2001, 414, 359-367.
9. K. Xu, *Chemical Reviews*, 2004, 104, 4303-4418.
10. W. H. Meyer, *Advanced materials*, 1998, 10, 439-448.
11. H. Hu, W. Yuan, H. Zhao and G. L. Baker, *Journal of Polymer Science Part A: Polymer Chemistry*, 2014, 52, 121-127.
12. Y. Zhang, Y. Zhu, G. Lin, R. S. Ruoff, N. Hu, D. W. Schaefer and J. E. Mark, *Polymer*, 2013, 54, 3605-3611.
13. H. Zou, S. Wu and J. Shen, *Chemical Reviews*, 2008, 108, 3893-3957.
14. J. Qiao, Y. Chen and G. L. Baker, *Chemistry of Materials*, 1999, 11, 2542-2547.
15. W. A. Gazotti, M. A. S. Spinacé, E. M. Girotto and M. A. De Paoli, *Solid State Ionics*, 2000, 130, 281-291.
16. Y.-C. Cao, C. Xu, X. Wu, X. Wang, L. Xing and K. Scott, *Journal of Power Sources*, 2011, 196, 8377-8382.
17. J. Nei de Freitas, A. F. Nogueira and M.-A. De Paoli, *Journal of Materials Chemistry*, 2009, 19, 5279.
18. D. E. Fenton, J. M. Parker and P. V. Wright, *Polymer*, 1973, 14, 589.
19. E. Quartarone, P. Mustarelli and A. Magistris, *Solid State Ionics*, 1998, 110, 1-14.
20. M. Anderman, *Solid State Ionics*, 1994, 69, 336-342.
21. S. T. Grajales, X. Dong, Y. Zheng, G. L. Baker and M. L. Bruening, *Chemistry of Materials*, 2010, 22, 4026-4033.
22. A. F. Nogueira, C. Longo and M. A. De Paoli, *Coordination Chemistry Reviews*, 2004, 248, 1455-1468.
23. J.-B. Kim, M. L. Bruening and G. L. Baker, *Journal of the American Chemical Society*, 2000, 122, 7616-7617.
24. J.-B. Kim, W. Huang, M. L. Bruening and G. L. Baker, *Macromolecules*, 2002, 35, 5410-5416.
25. J. Pyun, S. Jia, T. Kowalewski, G. D. Patterson and K. Matyjaszewski, *Macromolecules*, 2003, 36, 5094-5104.
26. L. Bombalski, K. Min, H. Dong, C. Tang and K. Matyjaszewski, *Macromolecules*, 2007, 40, 7429-7432.
27. W. A. Braunecker and K. Matyjaszewski, *Progress in Polymer Science*, 2007, 32, 93-146.
28. G. Moad, E. Rizzardo and S. H. Thang, *Australian Journal of Chemistry*, 2005, 58, 379-410.

29. G. Moad, E. Rizzardo and S. H. Thang, *Australian Journal of Chemistry*, 2006, 59, 669-692.
30. G. Moad, E. Rizzardo and S. H. Thang, *Australian Journal of Chemistry*, 2009, 62, 1402-1472.
31. C. Bartholome, E. Beyou, E. Bourgeat-Lami, P. Chaumont, F. Lefebvre and N. Zydowicz, *Macromolecules*, 2005, 38, 1099-1106.
32. C. Konn, F. Morel, E. Beyou, P. Chaumont and E. Bourgeat-Lami, *Macromolecules*, 2007, 40, 7464-7472.
33. C. J. Hawker, G. G. Barclay, A. Orellana, J. Dao and W. Devonport, *Macromolecules*, 1996, 29, 5245-5254.
34. C. J. Hawker, A. W. Bosman and E. Harth, *Chemical Reviews*, 2001, 101, 3661-3688.
35. A. C. Balazs, T. Emrick and T. P. Russell, *Science*, 2006, 314, 1107-1110.
36. T. von Werne and T. E. Patten, *Journal of the American Chemical Society*, 2001, 123, 7497-7505.
37. D. Sunday, S. Curras-Medina and D. L. Green, *Macromolecules*, 2010, 43, 4871-4878.
38. X. Jiang, G. Zhong, J. M. Horton, N. Jin, L. Zhu and B. Zhao, *Macromolecules*, 2010, 43, 5387-5395.
39. W. Yuan, H. Zhao, H. Hu, S. Wang and G. L. Baker, *ACS applied materials & interfaces*, 2013, 5, 4155-4161.
40. S. Saha, M. L. Bruening and G. L. Baker, *ACS applied materials & interfaces*, 2011, 3, 3042-3048.
41. K. Matyjaszewski, P. J. Miller, N. Shukla, B. Immaraporn, A. Gelman, B. B. Luokala, T. M. Siclovan, G. Kickelbick, T. Vallant, H. Hoffmann and T. Pakula, *Macromolecules*, 1999, 32, 8716-8724.
42. D. Li, G. L. Jones, J. R. Dunlap, F. Hua and B. Zhao, *Langmuir*, 2006, 22, 3344-3351.
43. M. K. Stowe, P. Liu and G. L. Baker, *Chemistry of Materials*, 2005, 17, 6555-6559.
44. Y. Chen, G. L. Baker, Y. Ding and J. F. Rabolt, *Journal of the American Chemical Society*, 1999, 121, 6962-6963.
45. E. Quartarone and P. Mustarelli, *Chemical Society reviews*, 2011, 40, 2525-2540.
46. M. A. Ratner and D. F. Shriver, *Chemical Reviews*, 1988, 88, 109-124.